Spiral spectrum of Airy–Schell beams through non-Kolmogorov turbulence

Yun Zhu (朱云)[1,2], Licheng Zhang (章里程)[2], and Yixin Zhang (张逸新)[2,*]

[1]*School of IoT Engineering, Jiangnan University, Wuxi 214122, China*
[2]*School of Science, Jiangnan University, Wuxi 214122, China*
**Corresponding author: zyx@jiangnan.edu.cn*

Received October 20, 2015; accepted January 25, 2016; posted online March 18, 2016

Based on the geometrical optics approximation, we analyze the effects of non-Kolmogorov turbulence on the spiral spectrum of the orbital angular momentum (OAM) of Airy–Schell beams. Our numerical results of Airy–Schell beams on the horizontal path show that the beam spreading due to diffraction is smaller for shorter wavelengths, a smaller OAM quantum number, a larger radius of the main ring, and a higher arbitrary transverse scale in weak turbulence. The oscillation frequency of the mode probability density of Airy–Schell beams in the radial direction is much lower than that of Hankel–Bessel beams. The mode probability densities of Airy–Schell and Hankel–Bessel beams are remarkably dependent on the wavelength and OAM quantum number. In order to improve the mode probability density, Airy–Schell beams with shorter wavelengths and lower OAM quantum numbers may be the better choice, which is diametrically opposite to Hankel–Bessel beams. Our research provides a reasonable basis for selecting light sources and precise tracking.

OCIS codes: 100.6640, 210.4770, 180.1790.
doi: 10.3788/COL201614.042101.

According to its exotic features, such as non-diffracting[1], self-accelerating[2–4], and self-healing[5,6] in vacuum, more and more attention has been paid to Airy beams. The propagation properties of Airy beams in atmospheric turbulence, such as scintillation[7,8], evolution[9], thermal blooming[10], beam wander[11], average intensity distribution[12], and average spreading[13] also have been carefully investigated. But, as we know, there are almost no discussions with respect to the effects of turbulence on the spiral spectrum of the orbital angular momentum (OAM) modes of Airy–Schell (AS) beams.

Considering the needs of precise tracking and significant deviations from Kolmogorov's model in certain atmospheric experiments[14], in this Letter, we discuss the radial distribution of the mode probability density (MPD) and crosstalk probability density (CPD) of the OAM modes of AS beams in the horizontal path through the non-Kolmogorov atmosphere in various situations. To reveal the distinctive properties of the spiral spectrum of the OAM of the AS beams in a turbulent atmosphere, we also compare them with Hankel–Bessel (HB) beams[15].

On account of the Gaussian-like Airy beam in far-field region, for long-distance transmissions, both truncated Airy and HB beams become spherical-like beams. Based on the Retov approximation, in the weak fluctuation region[16], $q = z/k\rho_{\mathrm{pl}}^2 < 1$, where $q\Lambda < 1$, ρ_{pl} is the spatial coherence radius of a plane wave, k is the wave number of light, and $\Lambda = 2z/kW^2$ is the Gaussian beam parameter characterizing the spot size W at the receiver. In the half-space $z > 0$, the complex amplitude of an Airy beam is given by

$$\mathrm{Ai}(r,\varphi,z) = \mathrm{Ai}_{l_0}(r,\varphi,z)\exp[\psi_1(r,\varphi,z)], \tag{1}$$

where $r = |\mathbf{r}|$, $\mathbf{r} = (x, y)$ is the two-dimensional position vector in the source plane, φ is the azimuthal angle, and z is the propagation distance. $\psi_1(r,\varphi,z)$ is the complex phase of waves propagating through turbulence and $\mathrm{Ai}_{l_0}(r,\varphi,z)$ is the normalized Airy-Gaussian model at the z plane with the OAM quantum number l_0 in free atmospheric turbulence. In the paraxial approximation, $\mathrm{Ai}_{l_0}(r,\varphi,z)$ has the form[17]

$$\mathrm{Ai}_{l_0}(r,\varphi,z) = -\frac{ik}{z}\omega_0(r_0-\omega_0 a^2)J_{l_0}\left(\frac{krr_0}{z}\right) \times \exp\left(ik\frac{r^2}{2z}+\frac{a^3}{3}\right)\exp(-il_0\varphi), \tag{2}$$

where ω_0 is associated with the arbitrary transverse scale, r_0 is the approximate radius of the main ring, and a is the exponential truncation. $J_{l_0}(krr_0/z)$ denotes the l_0^{th} order Bessel function of the first kind.

For a paraxial beam, the second-order cross-spectral density of the partially coherent case is defined by the statistical average over the ensembles as the following[16,18]:

$$W(r,r',z) = \langle E(r,\varphi,z)E^*(r',\varphi',z)\rangle, \tag{3}$$

where $E(r,\varphi,z)$ is the complex amplitude of the AS beams and $\langle\,\rangle$ represents the ensemble average of the source and atmospheric turbulence. In free space, Ref. [19] indicates that the normalized correlation function of Gaussian–Schell mode for any distance z is coincident with that of the original plane ($z = 0$). Based on the statistical independence between the sources and the atmospheric turbulence, the cross- spectral density of AS beams at any distance z is written as

$$W(r,r',z)=\langle \mathrm{Ai}(r,\varphi,z)\mathrm{Ai}^{*}(r',\varphi',z)\rangle_{\mathrm{at}}\mu(r,r',\varphi,\varphi'), \quad (4)$$

where $\langle\,\rangle_{\mathrm{at}}$ represents the ensemble average of the atmospheric turbulence. The last term of Eq. (4) is defined as the normalized correlation function of the Schell source and has the Gaussian form[19,20]

$$\mu(r,r',\varphi,\varphi')=\exp\left[-\frac{r'^2+r^2-2rr'\cos(\varphi'-\varphi)}{2\rho_s^2}\right],\quad \rho_s>0, \quad (5)$$

where ρ_s is the correlation radius of the Schell source at source plane $z=0$. By substituting Eqs. (1) and (5) into Eq. (4), we get

$$\begin{aligned}W(r,r',z)=&\,\mathrm{Ai}_{l_0}(r,\varphi,z)\mathrm{Ai}^{*}_{l_0}(r',\varphi',z)\\&\times\langle\exp[\psi_1(r,\varphi,z)+\psi_1^{*}(r',\varphi',z)]\rangle_{\mathrm{at}}\\&\times\exp\left[-\frac{r'^2+r^2-2rr'\cos(\varphi'-\varphi)}{2\rho_s^2}\right].\end{aligned} \quad (6)$$

By the quadratic approximation of the wave structure function, we can obtain the middle term on the right of the equals sign in the above formula as follows[16]

$$\begin{aligned}&\langle\exp[\psi_1(r,\varphi,z)+\psi_1^{*}(r',\varphi',z)]\rangle_{\mathrm{at}}\\&=\exp\left[-\frac{1}{2}D_{\psi}(r,r',z)\right]\\&=\exp\left[-\frac{r'^2+r^2-2rr'\cos(\varphi'-\varphi)}{\rho_0^2}\right],\end{aligned} \quad (7)$$

where $D_{\psi}(r,r',z)$ is the wave structure function, ρ_0 is the spatial coherence radius of a spherical wave, and the non-Kolmogorov turbulence is given by[21]

$$\rho_0=\left\{\frac{2(\alpha-1)\Gamma\left(\frac{3-\alpha}{2}\right)\left[\frac{8}{\alpha-2}\Gamma\left(\frac{2}{\alpha-2}\right)\right]^{(\alpha-2)/2}}{\sqrt{\pi}k^2\Gamma\left(\frac{2-\alpha}{2}\right)C_n^2 z}\right\}^{1/(\alpha-2)},\quad 3<\alpha<4, \quad (8)$$

where α is the non-Kolmogorov turbulence parameter, and $\Gamma()$ denotes the gamma function. C_n^2 is the generalized refractive-index structure constant over the path for horizontal homogeneous atmospheric propagation, characterizing the strength of the turbulence[16,22].

By combining Eqs. (6) and (7), we obtain the cross-spectral density of the AS beams

$$\begin{aligned}W(r,r',z)=&\,\mathrm{Ai}_{l_0}(r,\varphi,z)\mathrm{Ai}^{*}_{l_0}(r',\varphi',z)\\&\times\exp\left[-\frac{r'^2+r^2-2rr'\cos(\varphi'-\varphi)}{\tilde{\rho}_0^2}\right],\end{aligned} \quad (9)$$

where $1/\tilde{\rho}_0^2=1/(2\rho_{s0}^2)+1/\rho_0^2$, and $\tilde{\rho}_0$ is the effective spatial coherence radius for the AS beams, which includes the effects of the spatial coherence of the source and the correlated lengths of the phase fluctuations.

The function $E(r,\varphi,z)$ can be written as a superposition of the plane waves with phase $\exp(-il\varphi)$[23]

$$E(r,\varphi,z)=\frac{1}{\sqrt{2\pi}}\sum_l\beta_l(r,z)\exp(-il\varphi), \quad (10)$$

where l is the OAM quantum number and $\beta_l(r,z)$ is given by the integral

$$\beta_l(r,z)=\frac{1}{\sqrt{2\pi}}\int_0^{2\pi}E(r,\varphi,z)\exp(il\varphi)\mathrm{d}\varphi. \quad (11)$$

The radial distribution functions of the signal photons with the OAM quantum number l can be expressed as

$$\begin{aligned}\langle|\beta_l(r,z)|^2\rangle=&\frac{1}{2\pi}\int_0^{2\pi}\int_0^{2\pi}\langle E(r,\varphi,z)E^{*}(r',\varphi',z)\rangle\\&\times\exp[il(\varphi-\varphi')]\mathrm{d}\varphi\mathrm{d}\varphi'\\=&\frac{1}{2\pi}\int_0^{2\pi}\int_0^{2\pi}W(r,r',z)\exp[il(\varphi-\varphi')]\mathrm{d}\varphi\mathrm{d}\varphi'\\=&\frac{1}{2\pi}\int_0^{2\pi}\int_0^{2\pi}\mathrm{Ai}_{l_0}(r,\varphi,z)\\&\times\mathrm{Ai}^{*}_{l_0}(r',\varphi',z)\exp[il(\varphi-\varphi')]\\&\times\exp\left[-\frac{r'^2+r^2-2rr'\cos(\varphi'-\varphi)}{\tilde{\rho}_0^2}\right]\mathrm{d}\varphi\mathrm{d}\varphi'\\=&\frac{2\pi k^2}{z^2}\omega_0^2(r_0-\omega_0 a^2)^2\exp\left(\frac{2a^3}{3}\right)\\&\times\left|J_{l_0}\left(\frac{krr_0}{z}\right)\right|^2\exp\left(-\frac{2r^2}{\tilde{\rho}_0^2}\right)I_{l-l_0}\left(\frac{2r^2}{\tilde{\rho}_0^2}\right).\end{aligned} \quad (12)$$

We call $\langle|\beta_l(r,z)|^2\rangle$ the MPD of the signal photon in the case of $l=l_0$. For $l\neq l_0$, $\langle|\beta_l(r,z)|^2\rangle$ is defined as the CPD, which provides quantitative predictions for the integrity of free-space quantum communication systems[24,25].

In this section, we carry out a comparative study of HB beams, and in the horizontal homogeneous anisotropic channel, the MPD and CPD of AS beams through non-Kolmogorov turbulence as the functions of the radial position r in the output plane are shown in Figs. 1–7 with the parameters $z=1$ km, $l_0=1$, $\alpha=3.67$, $r_0=1$ mm, $\omega_0=0.01$ m, $a=0.05$, $\lambda=532$ nm, $C_n^2=10^{-16}$ m$^{3-\alpha}$, and $\rho_s=\infty$, unless otherwise indicated.

Figure 1 plots the MPD and CPD of the OAM for AS and HB beams versus the spatial correlation radius of the source ρ_s from 0 to 1 m for the different refractive index structure parameter C_n^2. From Figs. 1(a) and 1(c), it can be seen that the MPD of AS and HB beams for different C_n^2 increases steeply with the increase of the spatial correlation radius of the source ρ_s and tends to a stable value with further increase of ρ_s. Remarkably, the degradation induced by strong turbulence $C_n^2=10^{-14}$ (in the weak fluctuation region) is less significant when the spatial coherence of the beam is reduced. By comparing

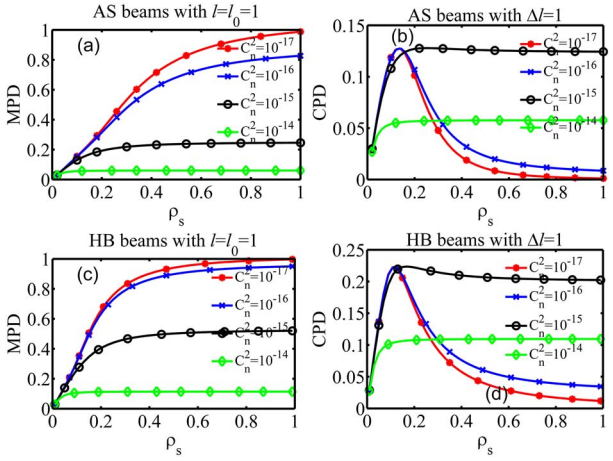

Fig. 1. MPD and CPD of AS and HB beams versus ρ_s for different values of C_n^2.

Fig. 1(a) with Fig. 1(c), the impact of the incoherence of the beam on the MPD of AS beams is greater than on HB ones, and the more incoherent the beam is, the greater the effects of turbulence on the OAM states of the beams are. Figures 1(b) and 1(d) show the CPD of AS and HB beams as the functions of the spatial correlation radius of the source ρ_s. For $C_n^2 < 10^{-15}$, the CPD first increases and then decreases, so it marked a peak value with increasing the spatial correlation radius of the source ρ_s. But for $C_n^2 > 10^{-15}$, the CPD increases first and then tends to saturation values. To summarize from Fig. 1, the single-mode transfer of fully coherent beams is superior to that of partially coherent beams. So in the following discussions, the fully coherent beam $\rho_s = \infty$ is adopted.

Figure 2(a) depicts the distribution of the MPD of AS beams along the direction of r for various l_0 with $l = l_0$. Figure 2(b) shows the CPD versus r for different Δl when $l_0 = 1$. Considering the symmetry of the Bessel functions for $l = l_0$, we discuss $l > l_0$ in the following. From Fig. 2(a), we can see that the MPD of AS beams decays with l_0 increasing. The peak values of the MPD $\langle|\beta_{l_0}(r,z)|^2\rangle$ move away from $r = 0$, and the widths of curves become wider as l_0 increases. For AS beams, a smaller l_0 may be the best option for communication. It is worth noting that in Fig. 2(b), as Δl gets larger, the peaks of the CPD of AS beams move outward and downward, while the minimum values of the CPD stay the same place for different Δl. Compared with HB beams, the opposite tendencies of the MPD $\langle|\beta_{l_0}(r,z)|^2\rangle$ of HB beams are observed. From Fig. 2(a)–2(d), one can see that as r increases, the MPD and CPD decrease. But the oscillatory curves of HB beams decay more quickly to zero compared to AS beams.

In Fig. 3(a), we display the variation of the MPD of AS and HB beams against r for selected wavelength $\lambda = 532$, 632.8, 850, and 1550 nm. Figure 3(a) illustrates that the shorter wavelength λ will give rise to a larger MPD of AS beams in the output plane. The variation tendency of the MPD and CPD of AS beams are the same for different wavelengths λ, but the amount of variation is different. The MPD and CPD versus λ with $r = 0.2$ are shown in the Fig. 3(b), which are similar to the results shown in Ref. [20]. As a comparison, the MPD and CPD of HB beams are illustrated in Figs. 3(c) and 3(d). Figures 3(c) and 3(d) show that the increasing λ will give rise to the broadening of the sub-ring of the MPD. Figure 3(d) also shows that the variation of the wavelength has relatively little impact on the CPD of HB beams.

Figure 4 reveals the relationship between the index α of non-Kolmogorov turbulence and the MPD or CPD of AS and HB beams. Considering that the dimensions of structure constant $C_n^2(z,\alpha)$ are dependent on exponent α for non-Kolmogorov turbulence, we adopt the generalized Rytov variance for a spherical wave as a constant[26,27] to discuss the effects of the index of non-Kolmogorov turbulence on the MPD and CPD of AS and HB beams. The generalized Rytov variance for a spherical wave is written as $\sigma_R^2 = -(2\alpha)^{-1} C_n^2 k^{3-\alpha/2} z^{\alpha/2} \cos(\alpha\pi/2) \cos[(\alpha-2)\pi/4] \times \Gamma(\alpha-1)\Gamma(\alpha/2)\Gamma[(2-\alpha)/2]\Gamma[(2+\alpha)/2]/\Gamma(\alpha)$[28]. In this

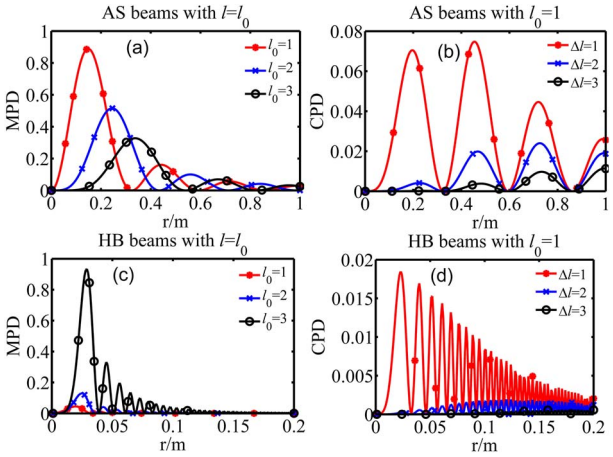

Fig. 2. MPD and CPD of AS and HB beams versus r for different values of l_0.

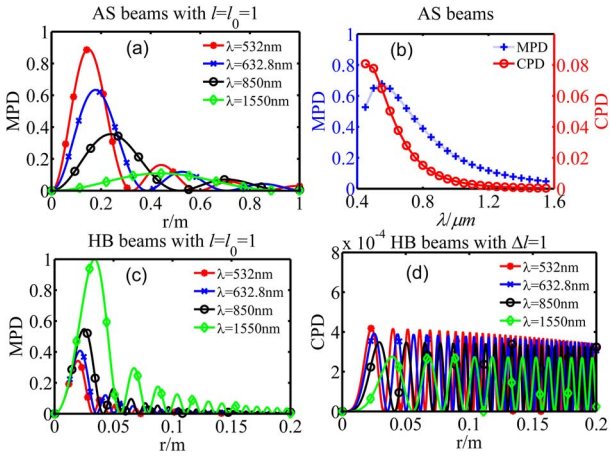

Fig. 3. MPD and CPD of AS and HB beams versus r with the different λ.

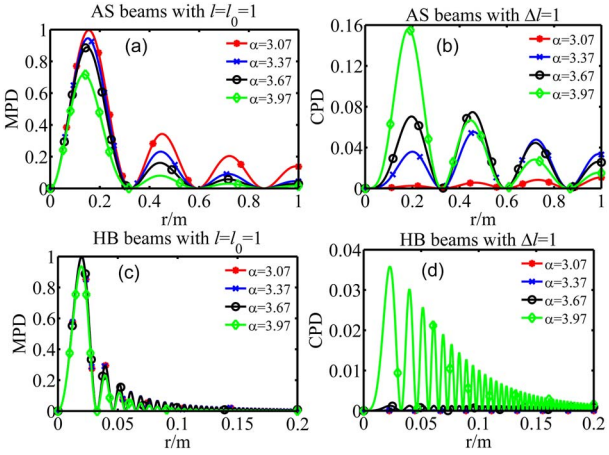

Fig. 4. MPD and CPD of AS and HB beams versus r for the different indexes α with $\sigma_R^2 = 7 \times 10^{-4}$.

Letter, we let σ_R^2 be a constant $\sigma_R^2 = 7 \times 10^{-4}$ ($C_n^2 = 10^{-16}$ m$^{3-\alpha}$ $\alpha = 3.67$), unless mentioned otherwise. Figure 4 indicates that the changing of index α of non-Kolmogorov turbulence has no impact on the radii of the main ring of beams in the output plane, whether the source beams are AS or HB ones. It can be seen from Fig. 4(a) that the larger α is, the faster the decay of the MPD is, and the peak positions of AS beams are closer to $r = 0$. Figure 4(b) illustrates that the CPD of AS beams decreases as the non-Kolmogorov parameter α increases for Δl. It is shown in Fig. 4(c) that the index α of non-Kolmogorov turbulence has a negligible impact on the mode probability of HB beams in the weak fluctuation region. It is also shown that the CPD of HB beams increases rapidly as α varies from 3.07 to 3.97. A smaller α will obtain a larger MPD in output plane, which is shown in Fig. 4.

Figure 5 shows the MPD and CPD of AS and HB beams as the function of r for different values of the refractive index structure constant C_n^2 with $\alpha = 3.67$. From Fig. 5, we can see that the ring widths of the MPD of AS beams or HB beams are independent of the value of C_n^2. Obviously, the larger the refractive index structure constant C_n^2, the smaller the MPD of the AS beams is. For HB beams, in Fig. 5(c), there is no influence of turbulence on the MPD for $C_n^2 = 10^{-17}, 10^{-16}$ m$^{3-\alpha}$. By further increasing the turbulence strength, the MPD of the HB beams begin to drop. The results of Fig. 5(d) show that the higher C_n^2 corresponds to the larger CPD at $\Delta l = 1$. For $\Delta l = 2$, further simulation indicates that the maximum value of the CPD of AS beams does not appear at the weak ($C_n^2 < 10^{-15}$) or stronger ($C_n^2 > 10^{-15}$) turbulence, but at the middle turbulence ($C_n^2 = 10^{-15}$).

Figure 6 plots the MPD and CPD of AS and HB beams as a function of r with the propagation distance varying from $z = 0.5$ km to $z = 1$ km. It is entirely reasonable that the MPD or CPD decreases as the propagation distance z increases. The CPD density of AS or HB beams is always symmetrical about $l = l_0$. It can be observed that the resilience against perturbations of turbulence disappears for the long propagation distance, then both AS and HB beams become Laguerre–Gaussian ones[29]. Using adaptive optics[30,31], the harmful effects of atmospheric turbulence for short distances can be tolerated or compensated.

Figure 7(a) displays that the truncation factor of AS beams has less impact on the MPD except for a truncation factor larger than 0.3, which agrees well with the fact that the Airy beams retain all their features for $a \ll 1$[5]. The changes of the MPD versus r are plotted in Figs. 7(b) and 7(c) with different radii for the main Airy ring r_0 and the arbitrary transverse scale ω_0. It is shown that the MPD increases as the main Airy ring r_0 increases, which is similar to the tendency reflected in radial scale ω_0. With the decrease of r_0, the curves of probability become flatter and the central positions go away from r_0, while radial scale ω_0 has no impact on the central positions of AS beams. Figures 7(b) and 7(c) show that beam spreading due to diffraction is smaller for larger r_0 and ω_0.

The change tendency of CPD is analogous to that of the MPD shown in Fig. 7; to avoid overly lengthy descriptions, the CPD is not plotted in Fig. 7.

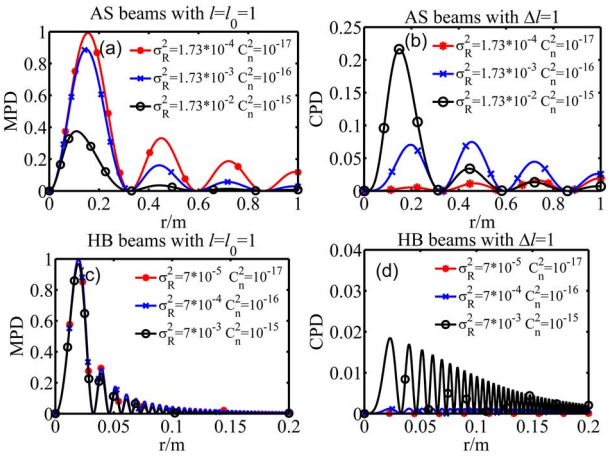

Fig. 5. MPD and CPD of AS and HB beams versus r for different C_n^2 with $\alpha = 11/3$.

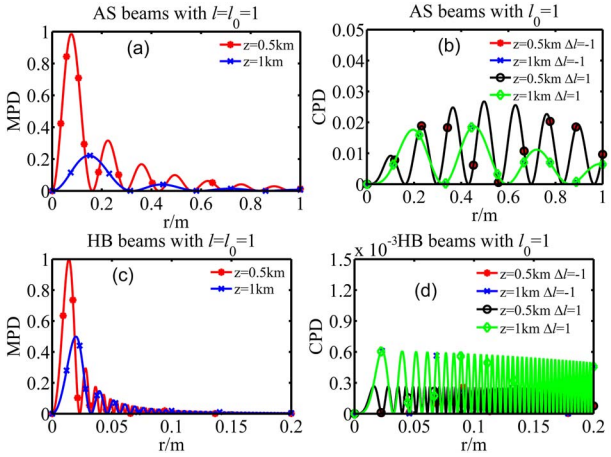

Fig. 6. MPD and CPD of AS and HB beams versus r when the propagation distance varies from $z = 0.5$ km to $z = 1$ km.

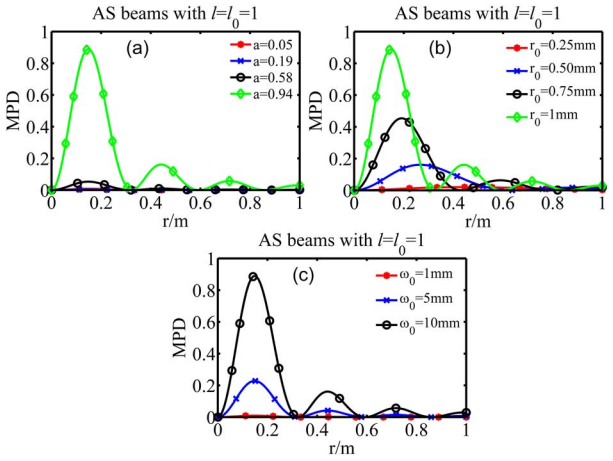

Fig. 7. MPD and CPD of AS beams versus r with different values of (a) the truncation factors a, (b) the radial positions of the main AS ring r_0, and (c) the radial scales ω_0.

In this Letter, the radial distributions of MPD and CPD in the z plane of the AS beams propagating through non-Kolmogorov turbulence are investigated in detail and are compared with HB beams. Our results indicate that in the weak fluctuation region, the single-mode transfer of fully coherent beams can exhibit a better performance than that of partially coherent beams. In the homogeneous anisotropic horizontal channel, the characteristics of the propagation of AS beams and all kinds of parameters tied closely to the transmission of the probability density distribution, CPD, and the peak positions of the MPD are analyzed. The results show that the peak positions of the MPD move away from $r = 0$ with the increase in the OAM quantum number l_0, wavelength λ, and the propagation distance z. However, they show the opposite trend when the non-Kolmogorov turbulence parameter α, the refractive index structure constant C_n^2, and the radius of the main Airy ring r_0 increase simultaneously. The MPD of AS is less affected for shorter wavelengths λ, smaller OAM quantum numbers l_0, larger r_0, and higher ω_0 in the weak fluctuation region. A larger MPD comes with a larger CPD in the vast majority of instances or vice versa. Compared with HB beams, the important difference is that the oscillation frequency of HB beams is much faster than that of AS beams. The MPD of AS and HB beams is remarkably dependent on parameters λ and l_0. HB beams with larger λ and l_0 may be the best choice, which is opposite to AS beams. Our research will serve as a theoretical underpinning for the precise tracking and design of an adaptive optics system that optically compensates for these turbulence effects on the OAM states of AS beams.

This work was supported by the Fundamental Research Funds for the Central Universities of China under Grant No. 1142050205135370.

References

1. M. V. Berry and N. L. Baazs, Am. J. Phys. **47**, 264 (1979).
2. I. M. Besieris and A. M. Shaarawi, Opt. Lett. **32**, 2447 (2007).
3. G. A. Siviloglou and D. N. Christodoulides, Opt. Lett. **32**, 979 (2007).
4. Z. Zhang, P. Zhang, M. Mills, Z. Chen, D. N. Christodoulides, and J. Liu, Chin. Opt. Lett. **11**, 033502 (2013).
5. J. Broky, G. A. Siviloglou, A. Dogariu, and D. N. Christodoulides, Opt. Express **16**, 12880 (2008).
6. X. Chu, G. Zhou, and R. Chen, Phys. Rev. A **85**, 013815 (2012).
7. H. T. Eyyuboğlu, Opt. Laser Technol. **47**, 232 (2013).
8. Y. Gu and G. Gbur, Opt. Lett. **35**, 3456 (2010).
9. X. Chu, Opt. Lett. **36**, 2701 (2011).
10. X. Ji, H. T. Eyyuboglu, G. Ji, and X. Jia, Opt. Express **21**, 2154 (2013).
11. W. Wen and X. Chu, J. Opt. Soc. Am. A Opt. Image Sci. Vis. **31**, 685 (2014).
12. C. Chen, H. Yang, M. Kayehrad, and Z. Zhou, Opt. Laser. Eng. **52**, 106 (2014).
13. R. Tao, L. Si, Y. Ma, P. Zhou, and Z. Liu, Opt. Laser. Eng. **51**, 488 (2013).
14. E. Golbraikh, H. Branover, N. S. Kopeika, and A. Zilberman, Nonlinear Processes Geophys. **13**, 297 (2006).
15. Y. Zhu, X. Liu, J. Gao, Y. Zhang, and F. Zhao, Opt. Express **22**, 7765 (2014).
16. L. C. Andrews and R. L. Phillips, *Laser Beam Propagation Through Random Media* (SPIE, 2005).
17. P. Zhang, J. Prakash, Z. Zhang, M. S. Mills, N. K. Efremidis, D. N. Christodoulides, and Z. Chen, Opt. Lett. **36**, 2883 (2011).
18. L. Mandel and E. Wolf, *Optical Coherence and Quantum Optics* (Cambridge University, 1995).
19. Q. He, J. Turunen, and A. T. Friberg, Opt. Commun. **67**, 245 (1988).
20. J. E. Morris, M. Mazilu, J. Baumgartl, T. Cizmar, and K. Dholakia, Opt. Express **17**, 13236 (2009).
21. Y. X. Zhang, Y. G. Wang, J. C. Xu, J. Y. Wang, and J. J. Jia, Opt. Commun. **284**, 1132 (2011).
22. T. Liu, P. Wang, and H. Zhang, Chin. Opt. Lett. **13**, 040601 (2015).
23. L. Torner, J. Torres, and S. Carrasco, Opt. Express **13**, 873 (2005).
24. C. Paterson, Phys. Rev. Lett. **94**, 153901 (2005).
25. G. A. Tyler and R. W. Boyd, Opt. Lett. **34**, 142 (2009).
26. M. Charnotskii, J. Opt. Soc. Am. A Opt. Image Sci. Vis. **29**, 711 (2012).
27. M. Charnotskii, J. Opt. Soc. Am. A **29**, 1838 (2012).
28. L. Tan, W. Du, J. Ma, S. Yu, and Q. Han, Opt. Express **18**, 451 (2010).
29. W. Nelson, J. P. Palastro, C. C. Davis, and P. Sprangle, J. Opt. Soc. Am. A Opt. Image Sci. Vis. **31**, 603 (2014).
30. J. Wang, J. Y. Yang, I. M. Fazal, N. Ahmed, Y. Yan, H. Huang, Y. X. Ren, Y. Yue, S. Dolinar, M. Tur, and A. E. Willner, Nat. Photonics **6**, 488 (2012).
31. N. Li, X. Lv, and C. Weng, Chin. Opt. Lett. **12**, 121103 (2014).